ASEG-PESA 2013
'THE EUREKA MOMENT'
11-14 AUGUST 2013 • MELBOURNE, AUSTRALIA

# Quality control of dipole acoustic data

**Marek Kozak**
*SuperSonic Geophysical LLC*
*35077 Donegal Ct. Newark CA, USA*
*marek@acousticpulse.com*

**Jefferson Williams**
*SuperSonic Geophysical LLC*
*906 Crestwood Terr. Los Angeles CA, USA*
*Jeff.Williams@acousticpulse.com*

## SUMMARY

Wave form excited by an acoustic dipole source in theory should consist of flexural waves only. Unfortunately usually it is contaminated by other acoustic modes including Stoneley, compressional wave and ringing casing. These undesired modes depend on the tool position inside the borehole, well deviation and its size, and presence of casing. Unwanted wave forms might be additionally augmented by poorly balanced dipole source and/or receivers. The classic semblance processing method will routinely deliver good looking results even when there are problems with one or more acoustic receivers and/or with poorly chosen processing parameters. Therefore I propose to add a complex wave form analysis as an additional quality control measure and to cross check the semblance method. Ways to identify a mixed acoustic mode condition and to eliminate biases in the shear slowness curves will be described. I also show how to qualify cross dipole data needed to perform shear wave anisotropy analysis.

**Key words:** dipole source; complex wave form analysis; shear wave anisotropy.

## INTRODUCTION

Acoustic wave generated by a dipole source and recorded by a wire line tool contains flexural wave propagating along the borehole wall. The flexural wave is used to derive shear wave slowness, formation mechanical properties (in combination with compressional wave), various directional parameters, fractures and shear wave anisotropy of surrounding strata. Dipole tools are typically operated under difficult conditions: excentralization, well deviation and rugosities, and washouts. Furthermore, dipole source might be misbalanced and excite not only flexural wave but also Stoneley and various higher order modes as well. The receivers may also underperform – due to poor calibration and/or the electronics failure.

Potential sources of flexural wave contaminations are:

1. Mixed acoustic mode condition.
   The most difficult to detect and correct for. Depending on the tool geometry and telemetry parameters it might be possible to observe the response on the opposite sides of the tool (e.g. separated angularly by 180 degree). It is the best and unequivocal method of identifying flexural wave as flexural waves are phase reversed while Stoneley or compressional waves travel in phase.

2. Formation shear wave anisotropy effects might further confuse the interpretation of dipole tool processing results.

3. Source and/or receiver misbalance.
   The responses recorded by the receivers should agree in phase and amplitude. Complex wave form analysis helps to resolve the issue of the receiver phase stability problems.

## METHOD AND RESULTS

Proposed complex wave form analysis used frequently to support and enhance classic semblance method consists of the following steps:

1. $Hn(t) = Im( Xn(t)), Re( Xn(t))$

   Hilbert transform delivers imaginary and real part of recorded wave forms (separately and independently at each receiver level).

2. $Pn(t) = Arctan[ Im(Hn(t))/Re(Hn(t))]$

   Phase arrivals are used to compute slowness across multiple receiver pairs.

3. $Sij(t) = 1/Z \ [Pj(t) – Pj(t)]$

   Symbol $Sij(t)$ denotes instantaneous slowness across receiver pair $ij$ for given time of $t$.

4. $dTij = 1/N \sum [Sij(t) \ dt]$

   The summing (or the integral range) is varying from the fastest possible shear wave slowness up to chosen upper limit which depends on the local formation properties. In above equation symbol N represents the number of integration points.

There are various benefits of enhancing semblance method by complex wave form analysis. The most important feature comes from the fact that phase analysis is based on individual receiver responses rather than statistics derived across entire receiver array. Thus complex wave form analysis is robust - even if one or more receivers fail, as long as there are at least four or five levels operating correctly, the final results will still be trustful. Furthermore, wave form data processed with semblance method will not deliver rich information about the tool stability and performance. Although the semblance peak value correlates to the quality of the data, it is relatively weak relation - computed slowness logs might still be contaminated.

**Flexural wave phase reverse effects**

Dipole source excited flexural wave should propagate with clear phase reverse observed on both sides of the tool (separated angularly by 180 degrees). Figure 1 shows typical wave forms recorded by the tool equipped with segmented receivers (four quadrants per the receiver level – two are presented). There are three clearly detectable parts of the wave train. The blue colour represents phase reversed flexural wave. The grey area corresponds to mixing the tail of the flexural wave with the front of Stoneley mode. The latest parts within the wave train are Stoneley waves. In case like this, when the well was vertical and the tool was correctly centralized, the wave form differentiation can be executed yielding enhancement of the flexural wave and reduction of Stoneley mode. Unfortunately when the toll is poorly centralized no differentiation should be performed – different travel times on both sides of the tool might generate severe phase distortions. Data need to be processed on each side separately. Furthermore, complex wave form analysis should be executed as it will detect potential phase problems due to tool sagging under highly deviated well condition.

**Dipole tools with differential recording geometry**

Data recorded with dipole tools that are based on automatic differentiation should be cross checked by executing both complex wave form analysis and slowness-frequency coherence technique. Figure 2 shows dispersive characteristic of flexural wave. Slowness shifts toward higher values following higher frequencies. This is quite unique pattern of propagating flexural wave. Similar observation can be made by analysing instantaneous frequency and slowness derived from complex wave form analysis.

**Effects related to shear wave anisotropy**

Figure 3 presents results obtained while processing dipole data using guided semblance and phase analysis. Track #1 shows flexural wave slowness logs – blue curve computed by semblance method versus brown curve generated by phase analysis. Track #3 represents instantaneous frequency across the receiver array. Track #4 – slowness distribution and Track #5 - semblance projection and its peak value. Instantaneous frequency shows two darker events – it is indication of fast and slow flexural modes that might be present within recorded wave train. Also, slowness distribution shows quite high level of scattering. This effect further supports previous conclusion.

In order to verify above observation the data were reprocessed using complex wave form analysis, with narrower time window applied. The reasoning is that if there are fast and slow flexural modes present in the wave train then narrower time window should reduce or eliminate double peaks seen on the instantaneous frequency track. Obviously the window was positioned at the same start time. Figure 4 shows obtained results. Instantaneous frequency is clean of double peaks, slowness distribution is less scattered, and slowness curves begin to show separation due to formation anisotropy.

The quality of the data recorded under anisotropic conditions might be further augmented by following procedural steps (see the Figure 5):

- On and off axis angular energy standard deviation (tracks #4 and #5 black curves) should remain less then few degrees.
- Post rotated phase distribution wave forms ought to show low level of scattering (tracks #2 and #3). The goodness curves should stay above 0.75 (black curves).
- Fast shear azimuth direction should be relatively study (magenta curve track#1).

**Receiver phase response effects**

Figure 6 presents “classic” log data obtained with dipole source under relatively fast formation conditions. Track #1 shows flexural slowness curves obtained by semblance (blue) and phase analysis (brown) while track #2 presents recorded gamma ray log. There are correlating very well with gamma ray. There is severe bias between them reaching in certain depth zones intervals 7%. Track #3 shows slowness distribution data – there is second strand of slowness events that are slower. Figure 7 shows the flexural wave move out – receiver level #4 is affected by severe phase shift malfunction caused very likely by electronic problems. The data were reprocessed using complex wave form analysis excluding receiver #4. The results are presented on Figure 8. Phase slowness distribution is clean (see the track #4). This error (approximately 4%) would have slipped unnoticed without executing complex wave form method.

## CONCLUSIONS

The proposed dipole acoustic data quality control procedure Should adopt following rules:

- In the case of dipole tools that are capable to record single side wave forms the phase reverse between both sides of the tool will assure that processed data originates from the flexural mode and not from unwanted Stoneley wave.
- If single side wave forms are unavailable then slowness-frequency coherence and/or instantaneous frequency analysis should be executed.
- Under anisotropic formation well conditions the average standard deviation of the fast shear azimuth ought to be less then few degrees.
- Also, the correlation across the angular energy distribution wave forms should be computed.
- Finally, complex wave form analysis should be performed parallel to the semblance method. It will help for early detection of anisotropic conditions. It will also allow identify and correct for receiver phase stability issues.

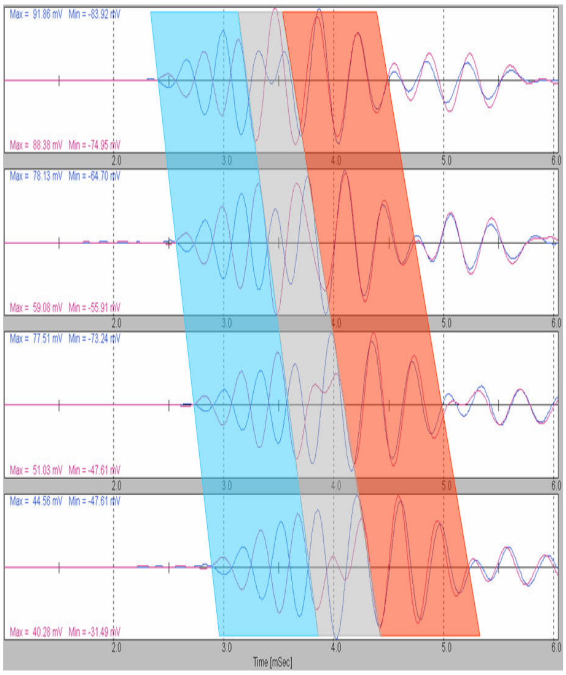

**Figure 1 Strong presence of mixed acoustic mode in dipole flexural data. Blue area shows phase reversed flexural arrivals. The grey zone represents mixed mode – the tail of the flexural wave is mixed with the front of slower Stoneley mode. The red part of the wave train corresponds to pure Stoneley arrivals (these are travelling in phase).**

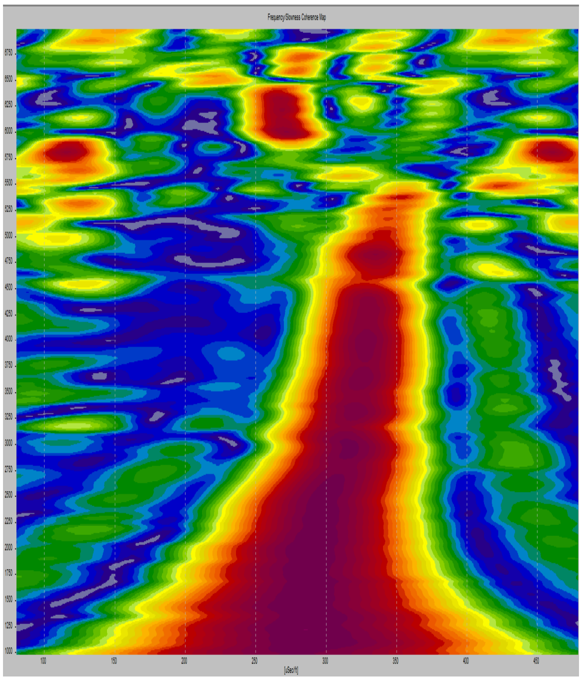

**Figure 2 Slowness-frequency coherence map computed in the absence of mixed acoustic modes. The vertical axis corresponds to the frequency while the horizontal represents slowness. Frequency dispersion characteristic shows faster slowness (associated with lower frequencies). This kind of frequency dispersion pattern characterizes flexural waves. Therefore in the absence of single side recording data (see Figure 1) frequency dispersion map could be used to qualify the flexural wave.**

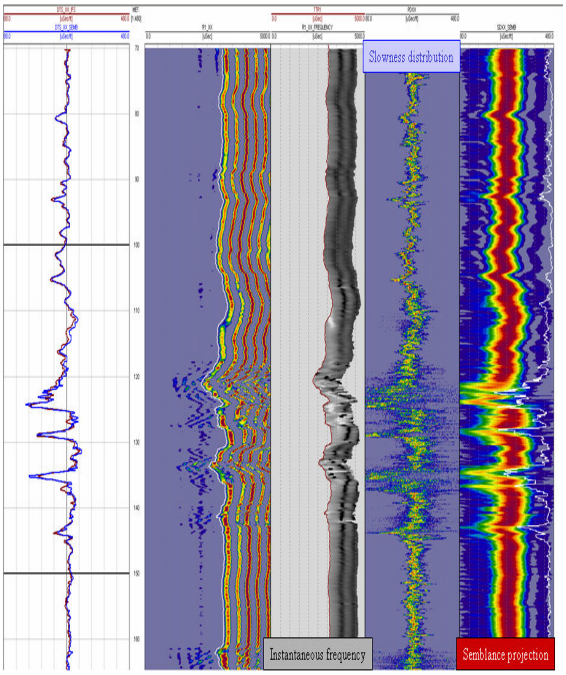


**Figure 3 Presence of mixed acoustic mode in dipole flexural data (shear wave anisotropy effects). Track #1 presents semblance slowness (blue) versus phase slowness (brown). Track #2 shows raw wave form data with arrival curve. Track #3 represents instantaneous frequency across receiver array. Track #4 – slowness distribution and track #5 – semblance projection.**

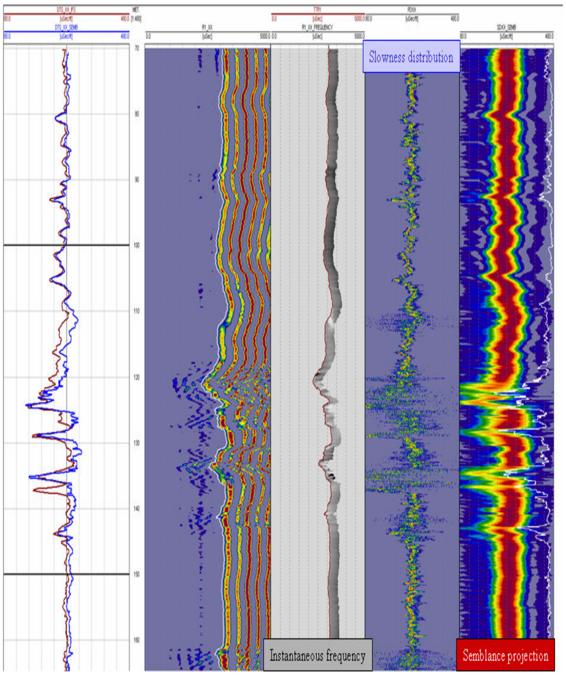


**Figure 4 In order to minimize mixing of fast and slow flexural wave the time window width of phase analysis was reduced down to 500 uSec. Slowness curves on track #1 show separations (semblance processing parameters were the same as presented on Figure 3).**

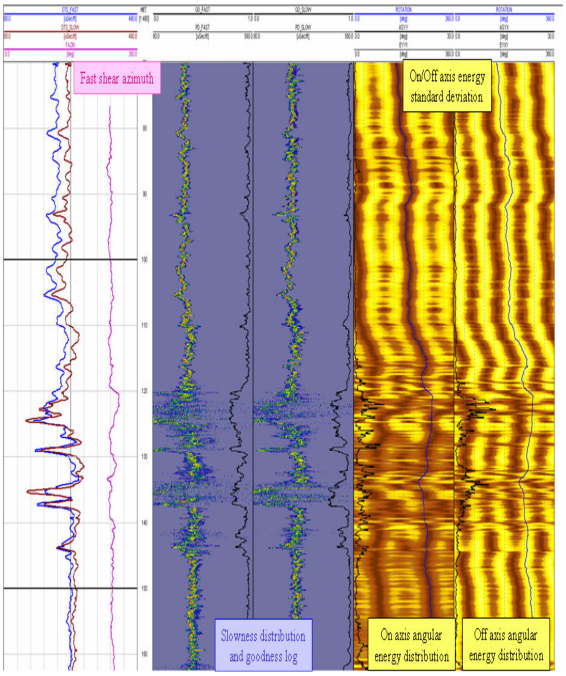


**Figure 5 Shear wave anisotropy analysis results. Track #1 shows fast flexural wave (blue), slow wave (brown), and fast shear wave azimuth (magenta). Tracks #2 and #3 present fast and slow wave forms distribution and associated goodness curves. Tracks #4 and #5 show on and off axis angular energy wave forms and their standard deviations. Rotation azimuth is shown as well.**

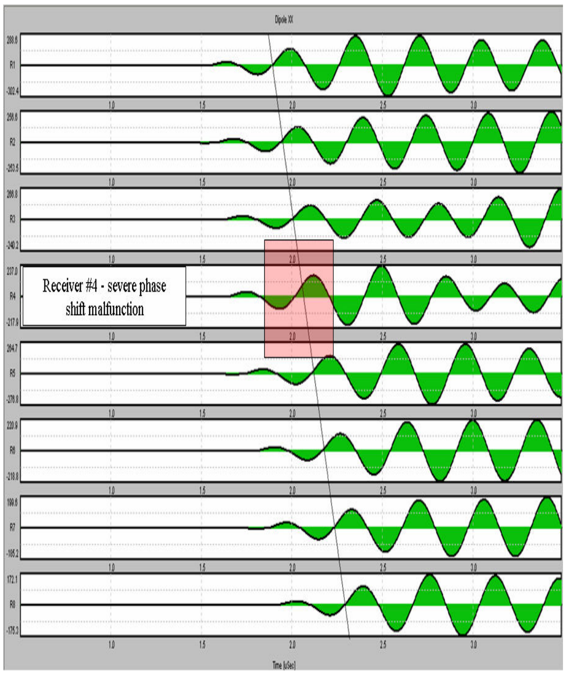


**Figure 7 Flexural wave forms move out. Receiver #4 is affected by severe phase shift malfunction. This type of failure will generate 4% error in slowness log computation and will likely slip unnoticed.**

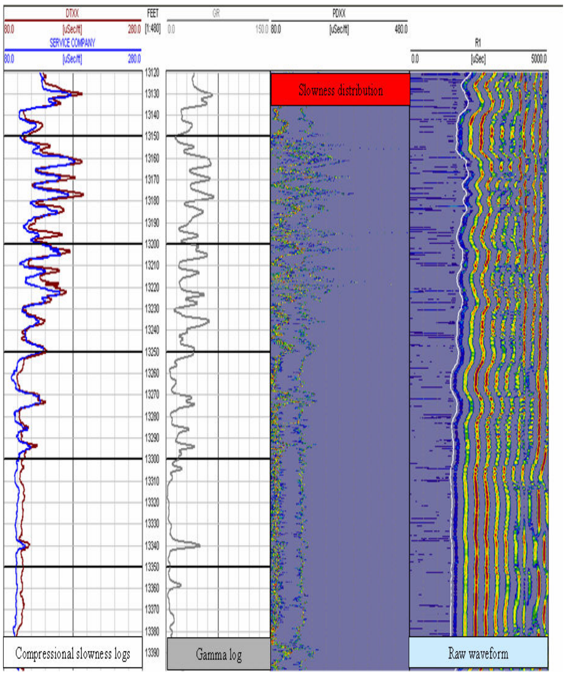


**Figure 6 Flexural wave processing results based on the semblance and complex wave form analysis methods. Track #1 shows semblance computed flexural wave slowness curve (blue) and the one computed by phase analysis (brown). Track #2 presents gamma ray log. Track #3 shows slowness distribution data. Track #4 prints raw flexural wave form with the arrival time recorded at near receiver level.**

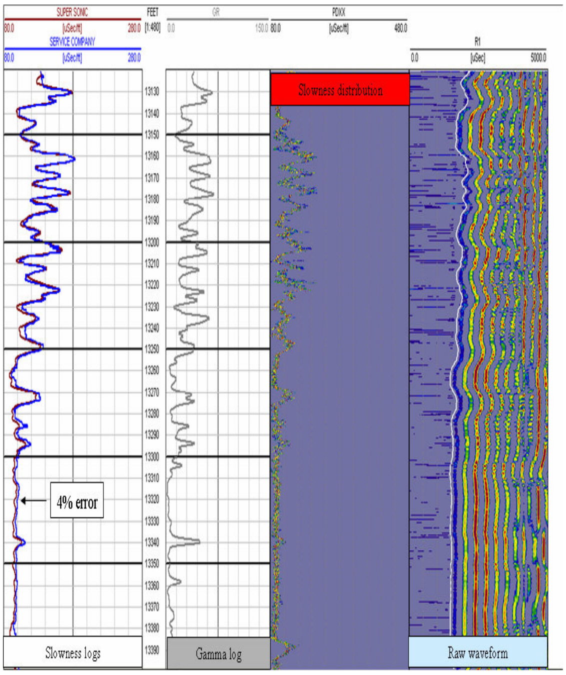


**Figure 8 Flexural wave processing results based on the semblance and complex wave form analysis methods. Track #1 shows semblance computed flexural wave slowness curve (blue) and the one computed by phase analysis (brown). The error with the receiver #4 included will be approximately 4%. Track #2 presents gamma ray log. Track #3 shows slowness very clean distribution data. Track #4 prints raw flexural wave form with the arrival time recorded at near receiver level.**